

## THE TRIGGER SYSTEM OF THE CHORUS EXPERIMENT

M. G. van Beuzekom, J. C. Boes<sup>1</sup>, E. A. van den Born, M. J. F. Jaspers, J. Konijn,  
R. G. C. Oldeman, C. A. F. J. van der Poel, T. van Reen, J. Stolte, J. W. E. Uiterwijk,  
J. L. Visschers:

**NIKHEF, Amsterdam, The Netherlands**

E. Pesen, M. T. Zeyrek:

**Middle East Technical University, Ankara, Turkey**

J. P. Dewulf:

**Inter-University Institute for High Energies (ULB-VUB), Brussels, Belgium**

F. Bal, R. Beyer<sup>2</sup>, P. Gorbunov<sup>3</sup>, R. Ferreira, B. Friend, M. de Jong<sup>4</sup>, L. Ludovici<sup>5</sup>,  
J. Panman:

**CERN, Geneva, Switzerland**

L. Bonnet, G. Gregoire:

**Université Catholique de Louvain, Louvain-la-Neuve, Belgium**

(To be submitted to Nucl. Instr. and Meth.)

### Abstract

A new apparatus for detection of  $\nu_\mu \rightarrow \nu_\tau$  oscillation has been successfully constructed and operated by the CHORUS Collaboration for the CERN-WA95 experiment. The design, implementation and performance of the electronic trigger system is described. A trigger efficiency of 99% was measured for  $\nu_\mu$  charged current events and 90% for neutral current events.

## 1 Introduction

The purpose of the CERN-WA95/CHORUS (CERN Hybrid Oscillation Research Apparatus) experiment is to search for neutrino oscillation in the  $\nu_\mu \rightarrow \nu_\tau$  appearance channel [1]. Search for neutrino oscillations in the  $\nu_\mu \rightarrow \nu_\tau$  sector is done by detecting the occurrence of the reaction  $\nu_\tau N \rightarrow \tau^- X$  in a background of

---

<sup>1</sup>Now at KPN, The Netherlands.

<sup>2</sup>Now at DESY, Hamburg, Germany.

<sup>3</sup>On leave of absence from ITEP, Moscow, Russia.

<sup>4</sup>Now at NIKHEF, Amsterdam, The Netherlands.

<sup>5</sup>On leave of absence from INFN Sezione di Roma, Rome, Italy.

$\sim 10^6$   $\nu_\mu$  induced charged- and neutral-current events. The  $\tau^-$  is identified by its charge and the decay kink in its muonic and hadronic decay modes accompanied with transverse momentum imbalance. A sensitivity of  $\sin^2 2\theta \sim 2 \times 10^{-4}$  at large  $\Delta m_{\mu\tau}^2$  is expected to be achieved with four years of data taking, corresponding to  $\sim 5 \times 10^{19}$  protons of 450 GeV/c accelerated by the SPS and delivered to a beryllium target to produce the Wide-Band Neutrino Beam [2].

In Fig. 1 the CHORUS apparatus is shown schematically. The experimental set-up is composed of an emulsion target, a scintillating fibre tracker system, scintillator trigger hodoscopes, an air-core hexagonal magnet, a honeycomb wire chamber, a lead/scintillating fibre calorimeter, and a muon spectrometer<sup>1</sup>. The target material consists of a total of 770 kg of nuclear photographic emulsion, in which the neutrino interactions are recorded. Nuclear emulsion provides three-dimensional spatial information with an excellent spatial resolution of the order of 1  $\mu\text{m}$ . The scintillating fibre system, together with the honeycomb wire chambers define particle tracks. The air-core magnet provide a means to measure the charge of low energy particles. The momentum and charge of hadrons can only be measured with the air-core spectrometer, while the muon momentum can also be measured with the magnetised-iron muon spectrometer. The total energy and the energy flow is measured with the calorimeter.

The trigger system of the CHORUS experiment is designed to select neutrino interactions in the emulsion target region. Its other important task is the synchronisation of data taking with the time structure of the neutrino beam. In each 14.4 s cycle of the SPS there are two spills of 6 ms, separated by 2.7 s. The main difficulties facing the trigger system are related to the need to form a strobe (i.e. a timing signal to synchronise logic decisions), since there is no incoming charged particle, and the limit of two events per neutrino spill, imposed by the opto-electronic system used to read-out the scintillating fibre tracker [4].

The trigger is designed to take fast decisions with high selectivity, while remaining versatile. In formulating the trigger requirements, limitations are set by available buffer size, the demand of tolerable dead-time losses and a minimal delay between interaction and trigger decision. The calorimeter and muon spectrometer also act as neutrino targets in which more than one hundred events per neutrino spill occur. Only about five of these are selected. A total of 16 different types of triggers can be recorded.

This paper gives a detailed description of the design, implementation and performance of the different parts of the complex trigger system of the CHORUS experiment. Particular emphasis is given to the trigger logic and tasks related to the synchronisation with the accelerator cycle. In addition to the oscillation search trigger, triggers for other physics purposes, efficiency studies and calibration will be described.

---

<sup>1</sup>The spectrometer together with its associated electronics (linear mixers, amplifiers and trigger logic) were part of the CDHS neutrino detector [3].

## 2 Trigger Hodoscopes and Veto System

The trigger system consist of scintillator planes. The counters are made of Bicon type BC-408 scintillator (polyvinyl toluene), with an attenuation length of more than 4 m. A 12 stage photo-multiplier tube (PMT) with a 2" diameter window is connected to the scintillator by means of a specially designed "adiabatic" light-guide. The PMT operating voltage is about 1800 V. The analog signal has a rise-time of 5 ns.

The configuration of the trigger hodoscopes is shown in Fig. 2. Table 1 summarises the trigger hodoscope characteristics. They are named E (Emulsion Plane), T (Timing Plane), H (Hodoscope), V (Veto) and A (Anti-counter).

### 2.1 The trigger scintillator systems

The E system is made of two staggered planes of seven, vertical, 20 cm wide scintillators. It is located 10 cm downstream of the 4th (most downstream) emulsion target ( $144 \times 144 \text{ cm}^2$ ), between fibre tracker planes 6 and 7, Fig. 1.

The T hodoscope system is made of two staggered planes of fifteen thin, 10 cm wide and 160 cm long, scintillator strips, coupled at both ends to a photo-multiplier and oriented horizontally. It is located behind the last fibre tracker plane. The thickness of the E and T hodoscope modules (6 mm per plane) minimises the loss of tracking precision due to multiple scattering, while maintaining a high efficiency.

The H hodoscope system consists of two staggered planes of twenty horizontal strips of 10 cm width and 200 cm length. It is positioned in front of the calorimeter. The width of T and H scintillator strips has been chosen to provide sufficient angular definition to separate tracks from interactions in the target (forward) and cosmic-rays and particles from interactions in the floor which make larger angles with respect to the beam direction.

A general staggering by one-half width was chosen in order to cover the dead space ( $\sim 1 \text{ mm}$ ) between two adjacent strips. The efficiency of each individual counter is continuously monitored, using beam-related muons, and was found to be better than 99%. The redundancy of two staggered planes ensures that, when a single strip is temporarily inactive, the loss of efficiency is at most 2%.

### 2.2 The veto system

The veto system V is installed 2 m upstream of the target region and consists of two staggered planes of twenty 20 cm wide scintillators oriented vertically (Fig. 2).

The distance between the veto system and target has been chosen to make it possible to avoid vetoes due to back-scattered particles from neutrino interactions in the target region by timing. The resolution of the time difference of a T and V

hit is sufficient to discriminate between forward and backward going tracks. The plane covers an area of  $3.2 \times 4 \text{ m}^2$ , large enough to screen beam related incoming muons and cosmic ray tracks which would satisfy the forward-direction criterion. The outer strips are oriented at an angle of  $13^\circ$  with respect to the central part of the plane, in order to fully cover the angular acceptance of the hodoscope trigger with minimal scintillator surface.

An additional anti-counter A system<sup>2</sup>, made of 2 planes of 16 scintillators 20 cm wide, vetoes events originating in the concrete floor upstream of the detector. It is positioned below the V plane and behind a 10 cm iron wall, which absorbs soft back-scattered particles.

The muon flux incident on the detector during the neutrino beam operation is  $N_\mu \sim 20 \text{ m}^{-2}$  per  $10^{13}$  protons on target. A veto inefficiency of  $1.5 \times 10^{-3}$ , provides sufficient rejection of beam related incoming muons.

### 2.3 Photo-multiplier Calibration, Timing Adjustment and Monitoring

The pulse height of the PMT signals is measured by 8 channel, 12 bit ADCs<sup>3</sup>, which can store 16 events with a digitisation time of  $16 \mu\text{s}$ . Eight PMTs are grouped into one ADC channel with linear mixers<sup>4</sup>. The charge is integrated within a 150 ns gate. To compensate for light attenuation, the PMT signal of the veto scintillator counters is amplified by a factor of 10 before the ADC conversion and the discriminator. Fig. 3 shows the typical ADC spectrum for minimum ionising particles.

A pulser system is used to calibrate and monitor the gain of each PMT of the T, V and H hodoscope systems<sup>5</sup>. It is based on green LEDs with a wavelength of  $557 \pm 10 \text{ nm}$ , delivering simultaneous light pulses of short duration (8 ns) to all PMTs. The pulse amplitude stability is 1%.

The timing is checked using 16 channel TDCs with multi-event (32 events) and multi-hit capabilities (16 hits/channel) and  $64 \mu\text{s}$  full dynamic range, with a double edge resolution of 20 ns and 1 ns time resolution<sup>6</sup>. The time measurement is made in common stop mode. A precision of 2 ns at FWHM per trigger scintillator of T and V hodoscopes is reached. This resolution is achieved by coupling the T and V scintillators strips at both ends to a photo-multiplier. Photo-multiplier signals are discriminated by a constant fraction discriminator with 200 ps time

---

<sup>2</sup>These scintillator counters are made of NE114 plastic and have already been used in the CHARM II experiment.

<sup>3</sup>Lecroy Research Systems, VME ADC Model No. 1182.

<sup>4</sup>Commercial NIM analog mixers and mixers specially designed at NIKHEF.

<sup>5</sup>“Calibrating and gain monitoring of the CHORUS PM’s”, NIKHEF/CHORUS internal note (1994); <http://choruswww.cern.ch/online/online.html>

<sup>6</sup>Lecroy Research Systems, VME TDC Model No. 1176.

walk<sup>7</sup>. A position independent signal is then provided by a 16 channel mean timer, allowing a maximum delay between first and second discriminator pulse of 50 ns and a timing resolution of 200 ps<sup>8</sup>. Furthermore, the TDC stop signal is provided by a programmable delay generator, with 24 bit dynamic range (170 ns - 16.7 ms), 1 ns resolution and 150 ps time walk<sup>9</sup>.

Fig. 4 shows a separation between tracks in the forward and backward direction of 13 ns at 1% of the peak value. This is enough to avoid false vetoes due to back-scattered particles from neutrino interactions in the target region.

Continuous monitoring of the trigger system is done by recording the signals of cosmic-ray muons in the time interval between accelerator cycles. A high-intensity 100 GeV/c muon beam is used for precise “time-zero” calibration at the beginning of every yearly data collection period.

The time response of all V-scintillator chains is equalised to within 0.5 ns using the comparison with an auxiliary long scintillator strip oriented horizontally to cross a maximum of V-strips. Once the whole V-plane is adjusted, it is used to define the timing for the smaller T-plane. The muon beam used for this timing adjustment illuminates the whole surface of the counter planes. A, E and H do not need a very precise time definition.

### 3 The oscillation search trigger

The trigger hodoscopes E, T, H, V and A are used to select neutrino interactions in the target and to reject background from cosmic rays, beam muons and neutrino interactions in the surrounding material outside the target, such as supports and the floor [5].

The  $\nu$ -trigger is defined by a hit coincidence in E, T and H planes and no activity in the veto system (V, A). The most simple trigger condition: a coincidence of T and H, vetoed by V has a rate of 1.4 triggers per  $10^{13}$  protons on target, unacceptably high for the two-event restriction of the opto-electronic read-out system. The combination of T and H strips requires consistency with a particle trajectory with  $|\tan\theta| < 0.20$  with respect to the neutrino beam. The track angle requirement reduces the  $\nu$  - trigger rate by about 30% without affecting the trigger efficiency. The events rejected by this requirement are mainly cosmic rays and events originating from the 16 cm thick iron floor.

After rejection of beam-related incoming muons, background events can still satisfy the trigger conditions if different tracks hit the different hodoscopes, thereby faking one small-angle track. These events are strongly reduced by minimising heavy support structures close to the trigger fiducial volume. Moreover,

---

<sup>7</sup>Lecroy Research Systems, CAMAC Constant Fraction Discriminator Model No. 3420.

<sup>8</sup>CAEN, Mean Timer Model C 561.

<sup>9</sup>Lecroy Research Systems, CAMAC QUAD, Programmable Gate and Delay control Model No. 4222.

the E hodoscope system, positioned as close as possible to the emulsion target and with an optimised surface area, eliminates neutrino interactions occurring in the iron support structure of the target region and image intensifier chains used in fibre tracker read-out. The net reduction in trigger rate by requiring the E plane in coincidence is 33% with respect to the above mentioned conditions. The anti-counter A hodoscope reduces further the trigger rate by 13%. It removes events generated in the concrete floor upstream of the detector.

The final trigger decision also requires that at least one calorimeter plane or one spectrometer magnet scintillator is hit. This condition improves the purity of neutrino induced events and further reduces the trigger rate by about 13%.

Including all these criteria the measured rate of  $\nu$ -triggers is 0.5 events per  $10^{13}$  protons on target, which implies an effective triggerable mass of 1700 kg, in good agreement with Monte-Carlo simulations [5]. Given an emulsion target mass of 770 kg and the mass of the fibre tracker material of 400 kg, the fraction of those interactions originating in the emulsion target is  $\approx 45\%$ .

## 4 The Trigger Logic

The trigger requirements are set by the available buffer size (16 events per spill due to limitation of ADCs) and tolerable dead-time losses (10% for a spill of  $10^{13}$  protons on target).

A trigger decision is made in four steps as shown in Fig. 5. Approximately  $10^3$  decisions have to be taken per spill and the total decision time per trigger is about 125 ns. The dead-time introduced by conversion of detector signals after a positive trigger decision depends on the type – for a trigger requiring opto-electronics read-out it is 120  $\mu$ s, while for the other triggers not requiring opto-electronic read-out it is only 20  $\mu$ s. A total of 16 different types of triggers are implemented for physics purposes, efficiency studies and calibration as explained in section 6.

### 4.1 First level trigger

The first step in the trigger logic consists of the formation of the strobe signal. A strobe is a timing signal needed to synchronise the decision logic. It replaces the beam-crossing signal in storage rings. In the case of a neutrino interaction in the emulsion target, the main trigger strobe is generated by a coincidence of a T plane signal, which defines the timing, and a H plane signal, with a rate of about 40 strobes per  $10^{13}$  protons on target. Both signals are a logical OR of the whole plane provided by a specially designed 48 ECL input VME-Logic OR Unit with an internal delay time of 7.5 ns and a time resolution better than 1 ns<sup>10</sup>.

---

<sup>10</sup>M. Ferrat, VME-Logic OR Unit, CERN-ECP (1993).

The strobe logic for the other triggers is made of coincidences of signals from the calorimeter and the spectrometer, which are combined (with a logic OR) with the main trigger strobe. The rate of the calorimeter and spectrometer strobe is about 300 counts per  $10^{13}$  protons on target. The calorimeter strobe has a jitter of 20 ns and the spectrometer strobe of 50 ns with respect to the precise main strobe. To make sure that the main trigger strobe provides the timing whenever it is present, the calorimeter and spectrometer strobe signals are delayed by their maximum jitter time.

The strobe signal provides the timing signal to start the pre-trigger, which makes a fast decision by checking a minimum set of conditions. For example, the main physics trigger requires a coincidence of the strobe with the neutrino spill gate and no activity in the veto planes.

The pre-trigger decision is made by a VME-Programmable Logic Unit (PLU), as described in Appendix A. A reset signal is provided if no pre-trigger condition is fulfilled. The reset time delay is therefore different for different stages of the trigger logic (Fig. 5): 25 ns for “no pre-trigger”, 125 ns for “no read-out”, and 135  $\mu$ s (20  $\mu$ s) for processing an emulsion (other) event. For “emulsion” events the CCDs of the opto-electronic chains are read out. This introduces a 15  $\mu$ s dead time to gate the micro-channel plate (MCP) and a 120  $\mu$ s dead time to shift the data from the light sensitive zone of the CCD to the memory zone.

The processing of a strobe signal introduces a 60 ns busy, even if no pretrigger was generated. This accounts for 10% of the total dead-time of the experiment.

## 4.2 Second level trigger and Main trigger decision

At this stage, low-level patterns are determined based on detector signals, like counting the number of planes for penetrating tracks, checking vetoes, applying fiducial volumes and so on. The main trigger decision is then initiated.

A complex chain of custom designed general purpose VME-Programmable Logic Units processes the decision on 16 ECL input signals (see Appendix A). The trigger condition for T and H scintillator planes is fulfilled by a particle trajectory consistent with  $|\tan\theta| < 0.20$  with respect to the neutrino beam<sup>11</sup>. The calculation is performed by a custom designed VME-Hodoscope Logic Unit (HODO), that accepts 30 T-inputs and 40 H-inputs, applies a logic matrix operation on the input patterns and generates corresponding output signals (Appendix B).

## 4.3 The final trigger decision

The sixteen final trigger pattern combinations are then calculated based on the second level trigger outputs and combined with another set of sixteen signals that control scale-down factors and use busy signals from the conversion electronics.

---

<sup>11</sup>The angle aperture of 200 mrad corresponds roughly to a width of five H scintillator strips.

The resulting 32-bit word is then transferred to a custom designed VME-Logic Matrix Unit (LMU) (Appendix C).

This module translates the 32 trigger decision inputs into 16 read-out signals, Fig. 6. Each bit in the 16 bit trigger pattern can generate a different read-out pattern, and each bit in the read-out pattern triggers a specific sub-detector. This technique allows for a different set of sub-detectors to be read-out for different triggers. For example, calorimeter and spectrometer triggers do not require the read-out of the opto-electronic subsystem.

Some triggers have to be validated by a specific “enable” signal to generate the corresponding read-out signal and thus can be down-scaled. The enable signal is switched on and off inside the spill by means of a VME-PLU, strobed by an internal timer (section 5.1), see Fig 6. The fraction of the time that the enable signal is on defines the pre-scaling factor desired.

#### 4.4 Consistency checks

To check the functioning of the decision logic, VME and CAMAC custom made 64 bit buffered pattern units (BPU) are used. Owing to the redundancy of information storage, self-checking is possible. For example, hit patterns stored in BPUs may be cross-checked against hit patterns recorded in HODO buffer memory on an event-by-event basis. Also, all inputs and outputs are latched and stored, and the consistency is checked at read-out for each event.

### 5 Synchronisation with accelerator cycle

As already mentioned above, in each accelerator cycle there are two 6 ms neutrino spills. A gate of 8 ms length is opened to contain each of the two spills. We refer to these as the “physics gates” (Fig. 7). Neutrino triggers are only accepted during the physics gate.

Another gate (“wide gate”) is also opened which fully contains the physics gate. It has a fixed length of 32 ms during which control measurements, such as dead-time digitisation, and the measurements of the field in the beam elements and hexagonal magnet are performed with a 10 kHz and 2 kHz frequency, respectively.

The data taking modes of the detector are synchronised to the accelerator cycle with the help of a hardware interrupt handler (CIRQ), described in Appendix D, and timing signals from the accelerator. All functions beyond the trigger decision are controlled by the software running on a dedicated CPU, described in section 7.



## 5.1 The timing system

A programmable timing system is used to set control signals and gates with a  $2\ \mu\text{s}$  granularity over a time period of maximum 131 ms ( $2^{17}\ \mu\text{s}$ ), see Fig. 8. This system consists of a pulse generator<sup>12</sup>, which in turn drives a scaler and a PLU. The scaler counts the number of pulses and presents this as a 16 bit pattern to its front panel. This pattern is used by the PLU as input pattern. The PLU is then programmed to produce control signals at programmable times within the maximum range of this system. The following signals are derived:

1. timing signal for pulsing the current of the hexagonal magnet;
2. control signals for dead-time calculation and beam spill time structure measurement;
3. control signals for digitisation of the field of the hexagonal magnet [6] and beam focusing elements;
4. “wide gate” start and stop signals;
5. “physics gate” start and stop signals;
6. various control signals (e.g., clearing cycle of CCD cameras [4]) and enable signals for the hardware.

## 5.2 The data taking cycle

During a neutrino spill the trigger processor has the control of the data taking operations. In the long period between neutrino spills control is given to the sub-detectors, which can take calibration events, each using a local trigger logic. Fig. 7 illustrates the timings provided by the global trigger in the course of each data taking cycle.

The synchronisation task running on the trigger system or local system CPU has two different modes: 1) supervisor mode - polling the inputs of the interrupt requester (CIRQ) during the neutrino spill; and 2) user mode - waiting for interrupts outside the neutrino spill. These modes correspond to the two main states: in-spill and out-spill. Fig. 9 shows the state machine diagram and corresponding sub-states [7], described below in detail.

### 5.2.1 Global data taking mode

The in-spill state consists of the following sub-states:

---

<sup>12</sup>CAEN, CAMAC - Preset Counter and Gate Generator, Model No C 423.

- Start of spill

When a spill synchronisation signal from the accelerator arrives (Fig. 8), an interrupt is generated and control is given to the trigger system, which runs in supervisor mode. In the spill initialisation phase, the status of all sub-detectors is checked. The physics gate is opened if all subdetectors are ready to take data.

- During physics gate

The trigger processor detects hardware trigger decisions by polling the status register of the interrupt handler. This gives a maximum latency of  $2 \mu\text{s}$ . At each trigger, the trigger conditions are read from the LMU and stored. If necessary, new trigger conditions can be set in the LMU within the conversion time of the subdetector signals. This allows one to impose a different event limit for each sub-detector, according to its buffer size. It allows the option of overlaying events in the CCD's image area by multiple opening of the MCP-gate. The software sets the new conditions within  $15 \mu\text{s}$  and does not contribute to the overall dead-time.

- End of physics gate

At the end-of-spill signal which is generated by the internal timer, all triggers are disabled, a list of event descriptors is sent to the event builder (EVB) and finally the task waits for the end of the read-out of the trigger system.

- Read-out state

In the read-out state the processor runs in user mode and interrupts are again enabled.

Events inside the neutrino spill are taken in a buffered mode. The digitised data in the buffers have to be uniquely identifiable, in order to be associated with the correct event. This is done with the help of a VME-Output Register<sup>13</sup> by storing for each event a 32 bit pattern in a Buffered Pattern Unit in each sub-detector. Each pattern is made up of event type (16 bit) and a quasi-random number (16 bit), the so-called “event tag”.

### 5.2.2 Local data taking mode

Local data can be taken at two different periods, Fig. 7: i) after the first spill, at the flat top of the accelerator (2.7 s), the so-called “west-hall” gate<sup>14</sup>; and ii) after the second spill, in the time interval between accelerator cycles (11.7 s).

---

<sup>13</sup>VME-Output Register, CERN-ECP (1993).

<sup>14</sup>The name is chosen to reflect the fact that during this period the SPS extracts its beam to the West-Hall. Muons from these other beam lines reach the neutrino detector and can be used for calibration purposes as well as leaving background tracks in the emulsions.

Calibration events are recorded one-by-one. These include cosmic-ray triggers in all sub-detectors as well as non-particle related events (flashing of fiducial fibres for calibration of opto-electronics, dummy gates for ADC pedestal determination), pulser events for PMT calibration of trigger scintillators and test triggers for general debugging of the hardware. This method allows independent and parallel recording of calibration triggers in all sub-detectors.

## 6 Other physics triggers

The task of the trigger is to select only the events relevant to the aims of the experiment. In addition to the neutrino interaction trigger in the emulsion target (main trigger) explained in section 3, several other triggers are implemented. The total number of triggers is about 5 per spill. The selections are based on the characteristics of the event, such as the presence of signals in the veto system, the location of the event vertex, the presence of long muon tracks in the calorimeter or spectrometer and the shower width and shower length. A detailed description of the trigger functions is given below; all rates are quoted for a spill of  $10^{13}$  protons on target. The typical intensity delivered on the target is between 1.0 and  $1.5 \times 10^{13}$  protons.

The **alignment trigger** selects muon tracks traversing the entire detector. Data with this trigger are taken at periodic intervals, in order to check the correct position relative to each other of all sensitive detector elements: emulsion trackers, scintillating tracking devices, streamer tubes, calorimeter and spectrometer. In this case the flexibility of the trigger system is fully exploited. The opto-electronic read-out chains consist of a four-stage image intensifier and a CCD camera [8]. The CCD sensor contains an image zone and a memory zone. The transfer time from the image to the memory zone is about  $125 \mu\text{s}$ , while the read-out of one image, done between neutrino spills or in between accelerator cycles, takes 20 ms per event. The Micro-Channel Plate (MCP) gate of the image intensifier ( $20 \mu\text{s}$  or less) is open for every alignment muon, but the transfer from CCD image zone to the memory zone is only made after four muons have been triggered and overlaid in one picture. In this way, eight alignment triggers can be taken per neutrino spill.

The **test beam trigger** is used for detector calibration. In the 2.7 s between the two neutrino spills, a secondary 120 GeV proton beam is delivered to the SPS West Area, producing tertiary pion, electron and muon beams. This is the “west hall” gate. For example, the energy inter-calibration between the emulsion target and fibre tracker and the calorimeter was done using a low energy pion beam in the “west hall” gate. At 7 GeV, the rate is 1.5 pions per  $2 \times 10^7$  protons extracted. The trigger is provided by a simple coincidence of a beam counter signal and the logical OR of the Veto plane V. When fewer than two neutrino events are recorded in the first spill, the corresponding physics gate is artificially extended into the

“west hall” gate allowing to take a maximum of two pion events. The physics gate is closed upon either hitting the CCD event limit, or the time-out occurring 1 s before the second spill, Fig. 7. In both cases, the events are treated like neutrino events as explained earlier. This technique allows to take calibration data with no loss of neutrino data taking.

A simple **strobe trigger**, consisting of a coincidence of the trigger counters T and H, was implemented to continuously monitor the detector efficiency. The original rate of  $\sim 40$  events per spill is down-scaled by a factor of 100 to 0.4 events per spill.

The **pilot target trigger** implemented for the RD46 experiment [9] is part of the CHORUS trigger system. A  $2 \times 2$  cm<sup>2</sup> and 1.8 m long capillary target is positioned upstream of the emulsion target. A neutrino interaction occurring in the capillary fibres fires a scintillator counter located downstream, which provides the respective trigger signal. In this case, both the pilot and main trigger bits are present at the input of the LMU. The data recorded in the pilot target is handled by a stand-alone data acquisition system running in parallel with CHORUS DAQ. The data are merged off-line with the help of the event tag (section 5.2.1). The rate is 0.01 events per spill.

The **calorimeter charged-current trigger** provides events for the study of neutrino-lead structure functions and beam flux measurements. The penetration condition requires a muon to penetrate at least two magnets of the muon spectrometer. The fiducial volume condition requires that the neutrino interaction takes place in the central upstream part of the calorimeter, corresponding to a target mass of 8.5 tons. The contamination of cosmic rays and beam muons together is about 1.5%. After down-scaling by a factor six, the event rate is about 0.5 per spill.

The **calorimeter two-track trigger** provides events for the study of charm physics. In addition to a penetration condition and a fiducial volume condition (target mass 26 tons) a two-track signal is required. The two-track signal can be fulfilled either by at least 3 calorimeter planes with exactly two hits or at least 2 spectrometer magnets with 2 hits or more. No down-scaling is needed, since the event rate is about 1 per spill. The efficiency of this trigger for charm production events was reported in [10].

The **quasi-elastic trigger** is implemented to record events with little hadronic activity, useful for measuring the neutrino energy spectrum. The fiducial volume and penetration conditions are the same as for the two-track trigger. Events with two or more hits in at least 3 calorimeter planes are vetoed, even so, inelastic charged-current interactions account for roughly 30% of the triggers, and a 10% contamination of cosmic-ray events has been measured. The event rate from this trigger is about 0.5 per spill.

The **neutral heavy lepton (NHL) trigger** is used to search for neutral heavy lepton particles. It exploits the large mass and detection capabilities of the calorimeter and spectrometer. The trigger requires the occurrence of a neutral

current interaction followed downstream by the decay or interaction of the heavy neutral particle. Between the first and second interaction point no hits must be detected, that is, a “hole” of more than two calorimeter or spectrometer planes must exist. In addition, low activity is required at the first interaction point. The rate is 0.02 events per spill.

An additional **long-lived neutral heavy-lepton trigger** is designed to detect NHLs produced in the muon spectrometer and decaying in the NOMAD neutrino oscillation detector [11], about 14 m downstream. It requires a coincidence (within  $\sim 100$  ns) of the **muon spectrometer minimum bias trigger** (MB) pattern and the pre-trigger signal  $T_1 \times T_2$  from the NOMAD detector, vetoed by a pack of 8 streamer tube planes located between the two detectors. The combination of the massive muon spectrometer and the relatively light and well instrumented NOMAD is suited for the NHL search in the mass range of 2-3 GeV. However, a regular implementation of this trigger in the framework of the logic described in section 4 turned out to be impossible due to a large delay of the NOMAD  $T_1 \times T_2$  signal. This was evaded by modifying the down-scaling mechanism of the “parent” spectrometer MB trigger, Fig. 6. In section 4.3 we explained that the down-scaling is done by the LMU at the final stage of the trigger decision. Early steps of the trigger decision introduce a delay during which the NHL coincidence signal has time to reach the LMU and override the down-scaling input. Therefore, the resulting trigger appears like a “tagged” spectrometer MB event. The streamer tube veto electronics has an adjustable “inefficiency”, for recording calibration CC events which constitute one third of the NHL trigger rate ( $\sim 0.25$ -0.3 events per spill). The CHORUS and NOMAD parts of NHL-events are recorded independently and assembled off-line, with the help of the synchronisation information the two detectors send to each other, once per SPS cycle, in the form of encoded pulse-trains. The timing of all relevant spectrometer and NOMAD signals is measured with 1 ns TDCs.

## 7 Trigger Data Acquisition System

The data acquisition system is designed according to the following requirements: sequencing the data taking with the accelerator cycle; read-out of the data stored in the front-end electronics; combination of the data into events; storage of the events on a storage medium; validation of the data; and interfacing to the user. A detailed description of the general CHORUS data acquisition system can be found elsewhere [1, 12]. We only present the aspects which are of particular interest to the trigger.

## 7.1 The trigger hardware

The CPU controlling the different trigger operations and communications with the event builder (EVB) is a commercial VME single board computer<sup>15</sup> with a 68040 processor and 32 Mbytes internal memory, running the OS-9<sup>16</sup> operating system [12]. The trigger system consists of 3 VME crates and 6 CAMAC crates interconnected via a VME Inter Crate (VIC) bus<sup>17</sup>, and 20 NIM crates for front-end analog and digital electronics. The bus drives the CAMAC crates using a Vertical Crate Controller<sup>18</sup>.

The CPU is used for the loading of the decision patterns in the various logic units (PLUs, Hodoscope unit, LMU) and for the setting of operational conditions in discriminators, pattern units, scalers, etc. It is also used for the control of the data taking (see section 5).

Monitoring and human interface is done with IBM RS-6000 workstations, connected with the VME system by Ethernet. The monitoring of the trigger hardware parameters, such as high voltages of the scintillator counters and low voltages of the crate power supplies, is done by the “slow control” system [13]. An alarm is issued if the measured values differ significantly from the values stored in the database. The slow control uses another OS-9 system to read-out the high speed CAENET<sup>19</sup> high voltage controllers. It reads the low voltages using a G64 system of multiplexed digital voltmeters, controlled with a VME processor connected to the G64 bus using a G64-VME bus interface<sup>20</sup>.

## 7.2 The trigger software

The trigger software was developed with the object oriented design paradigm, using the C++ programming language. A class library for all CAMAC and VME hardware modules was created. In addition, a set of different simple databases was implemented, including memory addresses, geographical locations in the VIC bus branch and parameter settings for hardware configuration. The computation of the complex trigger decision patterns is made on a UNIX machine, and loaded via Ethernet to the trigger CPU. This, in turn, loads them into the various CAMAC and VME based modules. The basic trigger conditions are stored in a database and can be modified dynamically through a graphical control panel implemented in the Tcl/Tk<sup>21</sup> language, running on a UNIX workstation. The

---

<sup>15</sup>VME Dual 68040 Fast Intelligent Controller, Model No. FIC-8234, CES, Switzerland.

<sup>16</sup>OS-9 System, Microware Systems Corporation, USA.

<sup>17</sup>VME Inter Crate, VIC to VME interface with Mirrored Memory, Model No. VIC-8251, CES, Switzerland.

<sup>18</sup>CAMAC Vertical Crate Controller, Model No. VCC 2117, CES, Switzerland.

<sup>19</sup>H.S. CAENET VME controller, Model No. V 288, CAEN, Italy.

<sup>20</sup>G64 - PEP Modular Computers, Switzerland. The G64 system was previously used in the CHARM II experiment.

<sup>21</sup>“Tcl and the Tk toolkit”, J.K. Ousterhout, Addison-Wesley, 1994.

lookup tables in the trigger hardware are refreshed at the start of each “run” (a period of typically 1 to 4 hours of data taking). The settings of the trigger decision parameters are stored in the normal data stream at the beginning of each run. Each change of condition is separately recorded in a simple database.

Online data monitoring and histogram display is done with the help of a dispatcher<sup>22</sup> - a message-based data distribution program, allowing the identification of malfunctioning channels (inactive or noisy).

Particularly important for the data collection efficiency of the experiment is the continuous monitoring of the event rates for triggers of various types, the associated dead-time values, the structure and timing of each neutrino spill as well as the muon flux in the shielding.

### 7.3 Data Volume

About 1 kbyte per event is recorded from ADCs, TDCs, BPU and PLUs. The beam related data and the information needed to calculate the dead-time of the experiment are stored in specially designed VME Buffered Scalers described in section 8.1. These data are read-out after each neutrino spill and have a volume of several kbytes. In addition, the integrated counting rate in all trigger scintillators is stored for each spill in commercial CAMAC scalars (a few kbytes).

The beam data banks include the time structure of neutrino spill, accumulated rates for normalisation purposes, beam symmetry information, the time-profile of the current in the hexagonal magnet, the magnetic field measurement from a Hall-probe as well as the currents applied to the wide-band neutrino magnetic focusing lenses (called “horn” and “reflector”) [2]. These three currents are digitised by an 8 channel Flash ADC (8 bit linear resolution) with a sampling rate of 2 KHz and stored in a 2 K deep memory<sup>23</sup>. Apart from monitoring purposes, the measurement of the hexagonal magnet current at the time of the event is important for charge identification of low momentum pions and muons. It is important to record the currents in the “horn” and “reflector” since they influence the spectra of the different flavours of neutrinos in the beam. Finally, data banks containing a description of read-out errors affecting the data quality are also recorded for each event.

## 8 Dead-time

The dead-time is the time required by the detector to process an event or take a decision after a strobe. The dead-time of the CHORUS experiment rises more

---

<sup>22</sup>Dispatcher - R. Gurin and A. Maslennikov, Proceedings of Prague Meeting 1995; <http://www-hep.fzu.cz/computing/HEPiX/HEPiX95/Overhead.html>.

<sup>23</sup>Struck Electronics for High Energy Physics and Industry, FADC-System, Model No. STR755 (FADC) and Model No. STR751 (Master)

than linearly with the beam intensity due to the two-event limit imposed by the CCD read-out. The linear term in the dead-time is inversely proportional to the effective neutrino spill length, which is defined as the length of an ideal squared-shaped neutrino spill which would give the same effective instantaneous rate<sup>24</sup>. A shortening of the neutrino spill length implies a relative increase of the duration of the event signal and thus of a larger dead-time<sup>25</sup>.

## 8.1 The dead-time measurement

The information used for the dead-time calculation, weighted with the neutrino spill structure, is stored in specially designed VME-Buffered Scalers with 2 K event deep memory<sup>26</sup>. This module has 4 clock inputs and 6 gate inputs. Each clock is gated with each individual gate, allowing 24 gate×clock coincidence signals to be recorded in as many scalars.

The muon rate in the beam, proportional to the neutrino flux, is measured inside the shielding. The number of passing muons are recorded with these scalars, gated with the wide gate, physics gate, and a ready-state of the detector during the physics gate for the various triggers. The rate is measured in time slices of 100  $\mu$ s, providing information on the neutrino spill time structure and time dependence of the dead-time. Fig. 10 shows a typical bell-shaped neutrino spill with a flat top to reduce dead-time.

The measured dead-time is less than 10% per effective spill of 4 ms and  $10^{13}$  protons on target. The main contributing sources are the CCD conversion and read-out (4.5%, including 3.3% caused by the maximum limit of two events<sup>27</sup>) and the ADC/TDC conversion time of about 20  $\mu$ s for an average rate of 5 events read-out per spill (2.5%). The activity in the veto counters and total strobe rate

---

<sup>24</sup>The effective neutrino spill is calculated as follows

$$t_{eff} = \frac{[\int_{t_1}^{t_2} (dN/dt) dt]^2}{\int_{t_1}^{t_2} (dN/dt)^2 dt},$$

where  $dN/dt$  is the instantaneous neutrino rate.

<sup>25</sup>The dead-time  $D$  is defined by

$$D = \frac{\text{Number of pulses} \times \Delta t}{t_{eff}},$$

where  $\Delta t$  is the duration of the signal.

<sup>26</sup>L. Bonnet, VME-Buffered Scaler Unit, Université Catholique de Louvain, Louvain-la-Neuve, Belgium, CHORUS Internal note (1994).

<sup>27</sup>This value is calculated assuming that the neutrino interaction rate obeys a Poisson distribution with an average of 0.5 events per spill and  $10^{13}$  protons on target. About 20% of the events with CCD read-out are taken as second event of this type. After the second event, a new CCD readout is not possible during rest of the spill. This dead-time is accounted as induced by the two-event limit and not as read-out dead-time.



account for about 1% dead-time.

The dead-time for the other physics triggers is less than 6%, but does not add directly to the previous sources since the signal conversion for these events is done during the busy time of the opto-electronic system.

The individual sources of dead-time per trigger type are also measured with a help of a VME Buffered Pattern Unit with 4 K deep event memory<sup>28</sup>. The input pattern, containing signals relevant for dead-time calculations, is latched by 100 ns long pulses generated by recording the timing of muons in small scintillators in the shielding of the neutrino beam<sup>29</sup>. Table 2 summarises the different sources of dead-time for a neutrino interaction in the target.

## 8.2 Double Events

Due to the long 15  $\mu$ s gate of the Micro-Channel Plate (MCP) of the image intensifier chain of the opto-electronic read-out and 50  $\mu$ s decay time of the phosphor used in these chains [4, 8], the effect of event overlays is important. Hardware was designed to enable double event identification by marking the presence of tracks during the long gating time.

The timing of every hit in the trigger scintillator counters is recorded for each event in commercial 16 channel VME-TDCs, described earlier. In addition, the hit pattern in all trigger scintillator planes is recorded in VME-Buffered Pattern Units for every strobe, formed by a simple coincidence of the T and H scintillator planes.

## 9 Trigger Performance

Table 3 summarises the statistics and data collection efficiencies of the CHORUS experiment for the period from 1994 to 1997. The reduction of main trigger rate per  $10^{13}$  protons on target, from 0.68 (1994) to 0.52 (1995), is due to the introduction of E plane in the trigger system. The increase in dead-time from 10% to 13% is related to the considerable increase in beam intensity delivered by the SPS accelerator, from  $\sim 1.0 \times 10^{13}$  to more than  $1.2 \times 10^{13}$  protons on target per neutrino spill. About  $2.3 \times 10^6$  events were collected of which  $7.9 \times 10^5$  charged current events originate in the emulsion target.

Owing to the high redundancy of the trigger system, a trigger efficiency of 99% was measured for  $\nu_\mu$  charged current events passing the off-line selection criteria. The corresponding efficiency for neutral current  $\nu_\mu$  interactions is 90%.

---

<sup>28</sup>L. Bonnet, VME-Buffered Pattern Unit, Université Catholique de Louvain, Louvain-la-Neuve, Belgium, CHORUS Internal note (1994).

<sup>29</sup>For a typical intensity of  $10^{13}$  protons on target and 4 ms effective spill, about 400 muons are measured inside the shielding by small scintillation counters. With pulses of 100 ns, this measurement has an inherent dead-time of its own of 1%.

Monte-Carlo simulation shows that the trigger efficiency for  $\nu_\tau$  interactions [5] is similar to the charged current trigger efficiency. The lower efficiency for neutral current events is due to low energy neutrino interactions, with large production of neutral particles ( $\pi^0$ 's) which deposit all their energy in the absorbing materials (emulsion, target trackers, streamer tubes) before reaching the calorimeter.

## 10 Acknowledgements

The realization of the trigger system of the CHORUS experiment was possible thanks to the contribution of numerous engineers and technical collaborators.

In particular we would like to thank: D. Bourillot, J. Dupraz, G. Roiron, G. Trouiller from the CERN staff for their help with the construction and installation of the trigger scintillator planes; H. Erdogan for his contribution to the adaptation of photo-tube bases at Middle East Technical University electric workshop and I. Dogru for his contribution to the production of light-guides at Middle East Technical University mechanical workshop; C. Gentet for her drawing support.

We gratefully acknowledge the financial support of the different funding agencies: The Scientific and Technical Research Council of Turkey (TUBITAK); The Foundation for Fundamental Research on Matter, FOM, and the National Scientific Research Organisation, NWO, in the Netherlands. Rui Ferreira thanks the financial support of JNICT - Junta Nacional de Investigação Científica e Tecnológica, PROGRAMA PRAXIS XXI, Lisboa, Portugal.

## References

- [1] E. Eskut et al., "The CHORUS experiment to search for  $\nu_\mu \rightarrow \nu_\tau$  oscillations", Nucl. Instr. and Meth. A401, 7 (1997) and references therein.
- [2] E. Heijne, CERN Yellow Report 83-06 (1983);  
G. Acquistapace et al., CERN preprint, CERN-ECP/95-14 (1995);  
L. Casagrande et al., CERN Yellow report 96-06 (1996).
- [3] M. Holder et al., Nucl. Instr. and Meth. A148, 235 (1978) and Nucl. Instr. and Meth. A263, 109 (1988).
- [4] S. Aoki et al., Nucl. Instr. and Meth. A344, 143 (1994);  
P. Annis et al., Nucl. Instr. and Meth. A367, 367 (1995).
- [5] E. Pesen, Ph.D. Thesis, Middle East Technical University, Ankara, Turkey (1997).
- [6] F. Bergsma et al., Nucl. Instr. and Meth. A357, 243 (1994).

- [7] P. J. Lucas, MSc Thesis, University of Illinois at Urbana-Champaign (1993).
- [8] M. Gruwé, Ph.D. Thesis, Université Libre de Bruxelles (1994);  
D. Rondeshagen, Dipl. Thesis, Westfälische Wilhelms-Universität (1994);  
C. Mommaert, Ph.D. Thesis, Vrije Universiteit Brussel (1995).
- [9] P. Annis et al., RD46 collaboration, Nucl. Instr. and Meth. A 360 (1995) 7.
- [10] K. Nakamura, Ph.D. Thesis in preparation, Osaka University, Japan (1998).
- [11] B. Schmidt, Ph.D. Thesis, Universität Dortmund (1997).
- [12] G. Carnevale et al., in “Procs. of CHEP’94 Conf.”, San Francisco, 1994;  
G. Carnevale, Laurea thesis, Università “Federico II”, Naples, 1995;  
F. Riccardi, Ph.D. Thesis, Università “Federico II”, Naples, 1996.
- [13] Slow Control System - D. Bonekämper, Dipl. Thesis, Westfälische Wilhelms-Universität (1993).

## Appendix A - Programmable Logic Unit (PLU)

The custom designed general purpose VME-Programmable Logic Units with high speed look up memories (12 ns) produce a decision based on 16 ECL input signals<sup>30</sup>. The unit has three different modes, controlled by the Control Status Register (CSR). This register is loaded through the VME bus. For the control logic, in addition to the strobe pulse, there is a Clear (CLR), a Load input (LD) and Synchronised output (SYNC).

In mode 1, the strobe latches the input data and generates the corresponding ECL output signals within 20 ns. The output levels are valid for the duration of the strobe, and go to zero after that. The SYNC signal flags the validity of the outputs.

In mode 2, the strobe latches the input data like in mode 1, but the data and SYNC outputs are reset by a signal on the CLR input.

In mode 3, the strobe latches the input data like in mode 1 and 2, but the reset is internally. The reset delay is adjusted by setting a register over the VME bus.

The load input stores the latched input and output data into a 1K deep buffer memory, that can be read and written over the VME bus.

## Appendix B - Hodoscope Logic Unit (HODO)

The custom designed special purpose VME-Hodoscope Logic Unit<sup>31</sup>. accepts 32 A-inputs and 40 B-inputs, applies a logic matrix operation on the input patterns and generates an output signal whenever a predefined condition is fulfilled.

Each true B-input generates internally a 32 bit vector. The value of this vector is programmable arbitrarily. A logic bit-by-bit OR is performed on the 40 vectors. The resulting 32 bit vector is used as a “mask” to be compared with the 32 A-inputs. If the bit-by-bit AND of the 32-bit result vector and the 32 bit A-input vector is non-zero, the module generates a “true” output value. The operation of the unit with respect to strobe and load inputs are similar to the situation in the PLU.

Only 30 out of 32 A inputs are used in the CHORUS trigger.

---

<sup>30</sup>J.P. Dewulf, “Programmable Logic Unit”, Inter-University Institute for High Energies (ULB-VUB), Brussels, Belgium, CHORUS internal note (1994).

<sup>31</sup>J.P. Dewulf, “Hodoscope Logic Unit”, Inter-University Institute for High Energies (ULB-VUB), Brussels, Belgium, CHORUS internal note (1994).

## Appendix C - Logic Matrix Unit (LMU)

The custom designed VME-Logic Matrix Unit<sup>32</sup> translates 32 trigger decisions into 16 read-out signals. The conversion is implemented with four eight-bit look-up tables, each producing a 16-bit result vector. The output is the bit-wise OR of the four 16-bit result vectors. Like the VME-PLUs, the module works in latch mode with a propagation delay from the front panel input to the output of less than 20 ns. Both the ECL inputs and ECL outputs are maskable through a register written over VSB or VME, and both the latched input (before mask) and output (after mask) pattern can be read over VME and VSB.

The module operates in two different modes: Acquisition and Bus mode. Switching between these modes is done on the software level by accessing the Control Status Register. In Acquisition mode front panel operation is enabled and a limited number of commands is allowed. In Bus mode front panel operation is disabled and all commands are allowed.

## Appendix D - Interrupt Request Module (CIRQ)

The CIRQ module accepts 6 interrupt sources (NIM or ECL) of a minimum width of 10 ns<sup>33</sup>. The inputs can be selectively enabled. When the unit is in a state to accept inputs, an input generates a corresponding busy signal. Depending on a second mask register, such a specific busy signal can generate a common busy signal. Depending on a setting in the status register a common busy signal sets in turn the interrupt request on the VSB or VME bus. The busy states can only be reset via the VME or VSB bus.

The different features are enabled by setting the appropriate bits in the Control Status Register. A special register is provided to clear the interrupt and the busy signals, or to generate a software controlled interrupt. Finally, there is a Data Register to read-out a 32 bit data pattern from the front panel. These ECL data inputs signals are latched into a buffer memory, whenever a common busy signal is generated.

---

<sup>32</sup>M. van Beuzekom, J. L. Visschers, J. Stolte and T. van Reen, "Logic Matrix Unit", NIKHEF, Amsterdam, The Netherlands, CHORUS internal note (1994); <http://choruswww.cern.ch/online/online.html>

<sup>33</sup>F. Bal, VME/VSB Interrupt Request Module, V451-CIRQ, CERN-ECP/EDA/DQ (1992).

Trigger Hodoscope	E	T	H	V	A
# strips/plane	7	15	20	20	16
Strip width (cm)	20	10	10	20	20
Strip length (cm)	148	160	200	320	200
Number of planes	2	2	2	2	2
Area covered (cm <sup>2</sup> )	150×148	160×160	200×200	400×320	200×320

Table 1: Characteristics of trigger hodoscopes.

Dead-time source	Rate/spill	Length	Dead-time (fraction)
Veto	400	70 ns	$7 \cdot 10^{-3}$
Pre-trigger	40	125 ns	$1 \cdot 10^{-3}$
Strobes from other detectors	300	60 ns	$5 \cdot 10^{-3}$
MCP gate	0.5	15 $\mu$ s	$2 \cdot 10^{-3}$
CCD conversion	0.4	120 $\mu$ s	$12 \cdot 10^{-3}$
Maximum limit of two events	-	-	$33 \cdot 10^{-3}$
ADC/TDC conversion	5	20 $\mu$ s	$25 \cdot 10^{-3}$
Total			$85 \cdot 10^{-3}$

Table 2: Contribution to event losses by dead-time for a 4 ms effective spill at  $10^{13}$  protons on target. The dead-time measured in the experiment is usually larger due to a shorter effective spill and a higher intensity achieved.

	1994	1995	1996	1997
Protons on target (pot) / $10^{19}$	0.81	1.20	1.38	1.66
Data collection efficiency	77%	88%	94%	94%
Total dead-time	10%	10%	13%	12%
Main trigger rate / $10^{13}$ pot	0.68	0.52	0.48	0.46
Emulsion triggers	422,000	547,000	620,000	720,000

Table 3: Summary of data collection statistics of the CHORUS experiment.

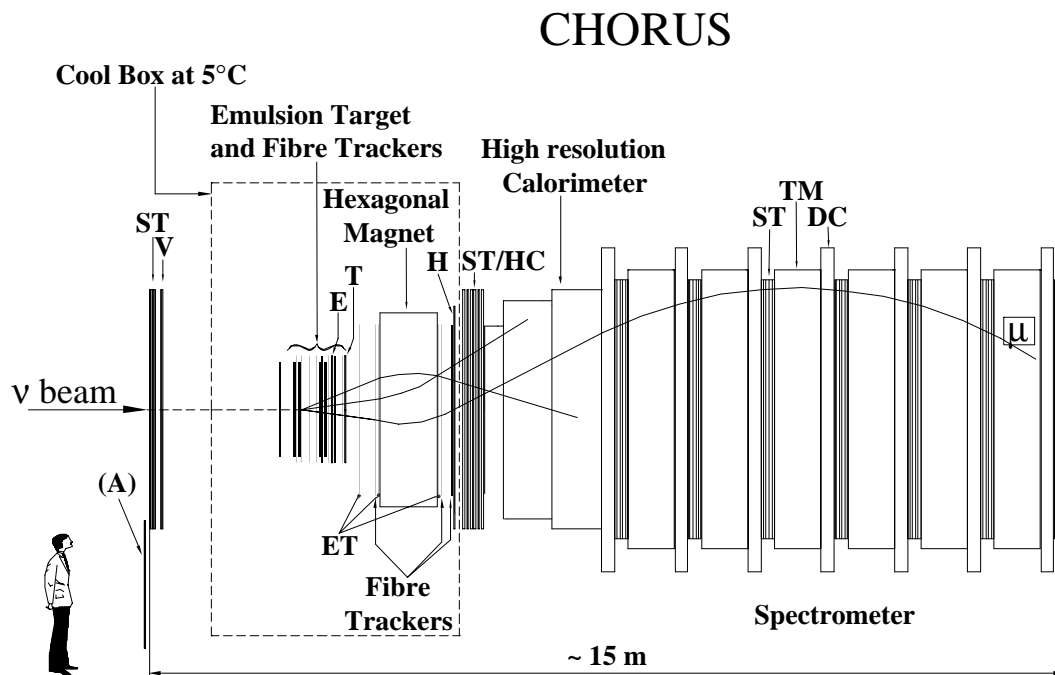


Figure 1: The schematic diagram (side view) of the CHORUS hybrid detector, showing the location of the different trigger and veto hodoscopes denoted by V, A, T, E and H. ST, TM and DC stands for streamer tubes, iron toroidal magnets and drift chambers, respectively, of the muon spectrometer system. The emulsion trackers and honeycomb chambers are denoted by ET and HC, respectively.

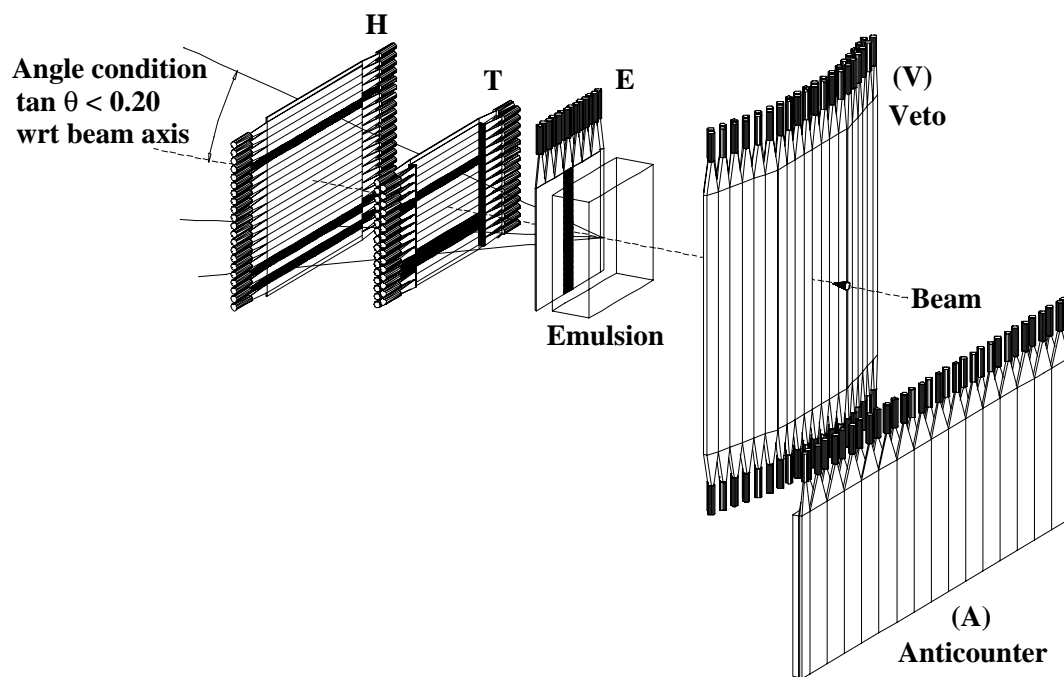


Figure 2: Schematic view of the trigger hodoscopes, illustrating a neutrino interaction in the emulsion target.



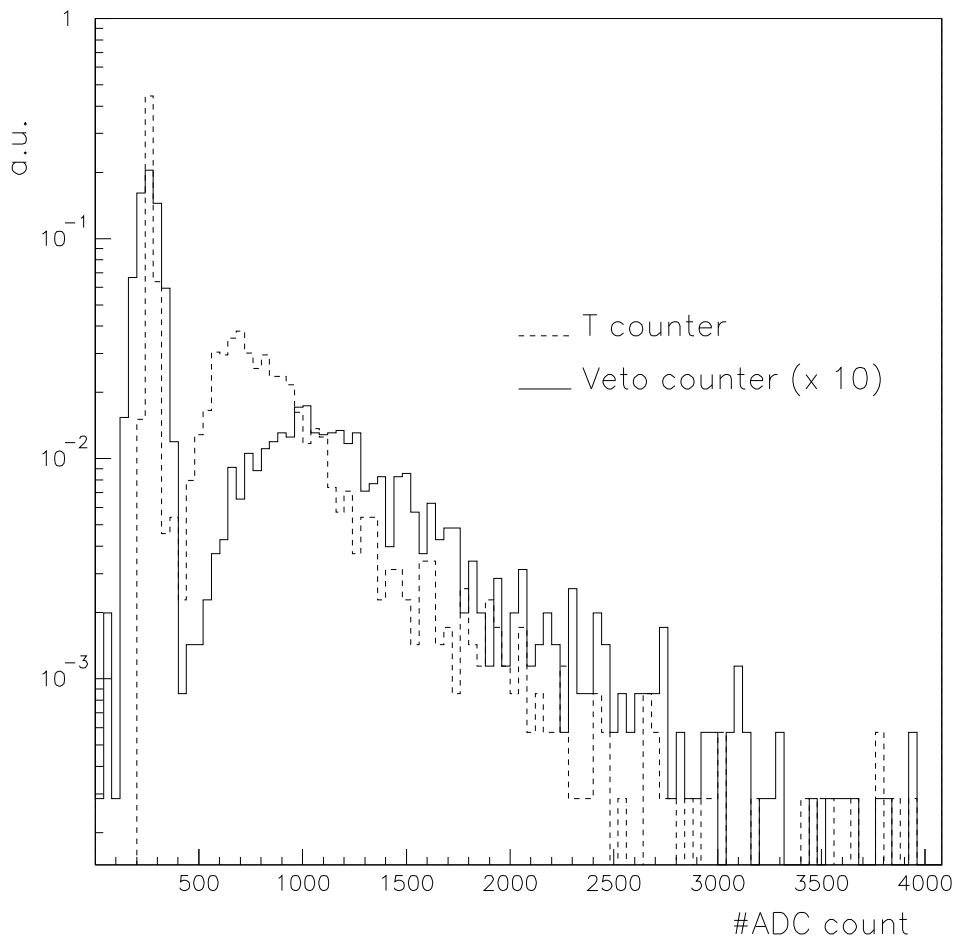


Figure 3: Typical ADC spectrum for minimum ionising particles hitting a V and T scintillator counter. The first peak in the spectrum is the pedestal.

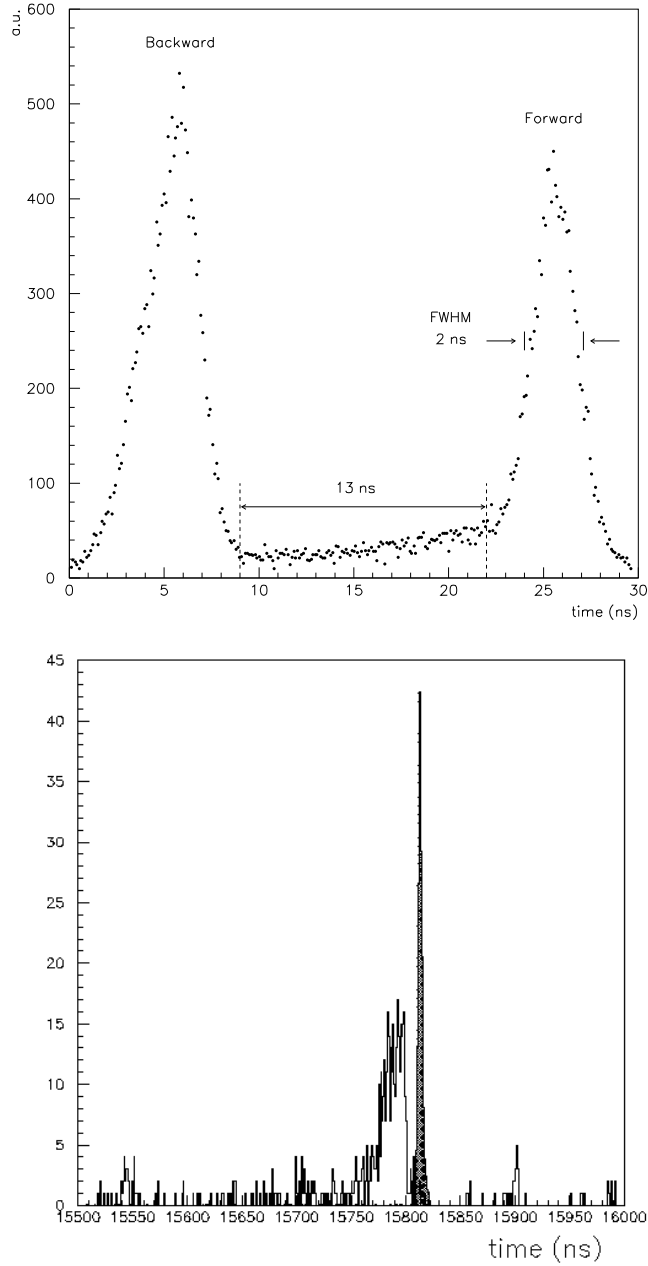


Figure 4: The forward-backward time distribution for cosmic muons (top). The measured time correlation between hits in trigger plane T and veto plane V during neutrino spills (bottom). The shaded peak is due to beam related muon tracks, while the events at smaller time values are mainly from back-scattered particles in neutrino interactions in the target region, which can clearly be separated. The time is measured in the V plane expressed in ns before the common stop provided by the T-hit.

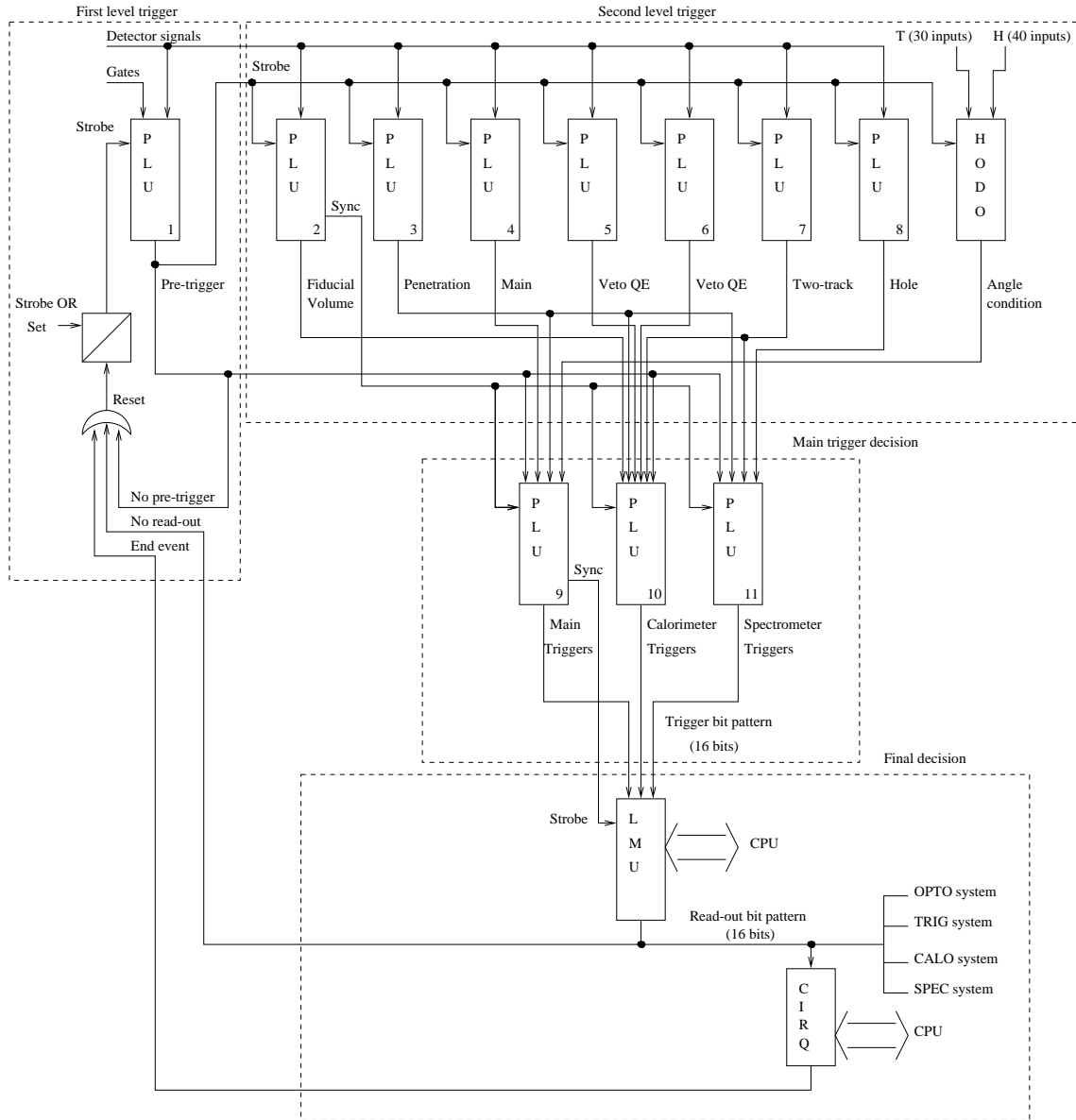


Figure 5: Schematic diagram of the four different levels of the trigger logic. Main triggers include main oscillation search trigger, auxiliary trigger, pilot trigger, strobe trigger, random trigger, pulser trigger and alignment trigger. Calorimeter triggers consist of minimum bias trigger, charged current trigger, dimuon trigger and quasi-elastic trigger. Spectrometer triggers are formed by minimum bias trigger, charged current trigger, dimuon trigger and neutral heavy-lepton trigger.

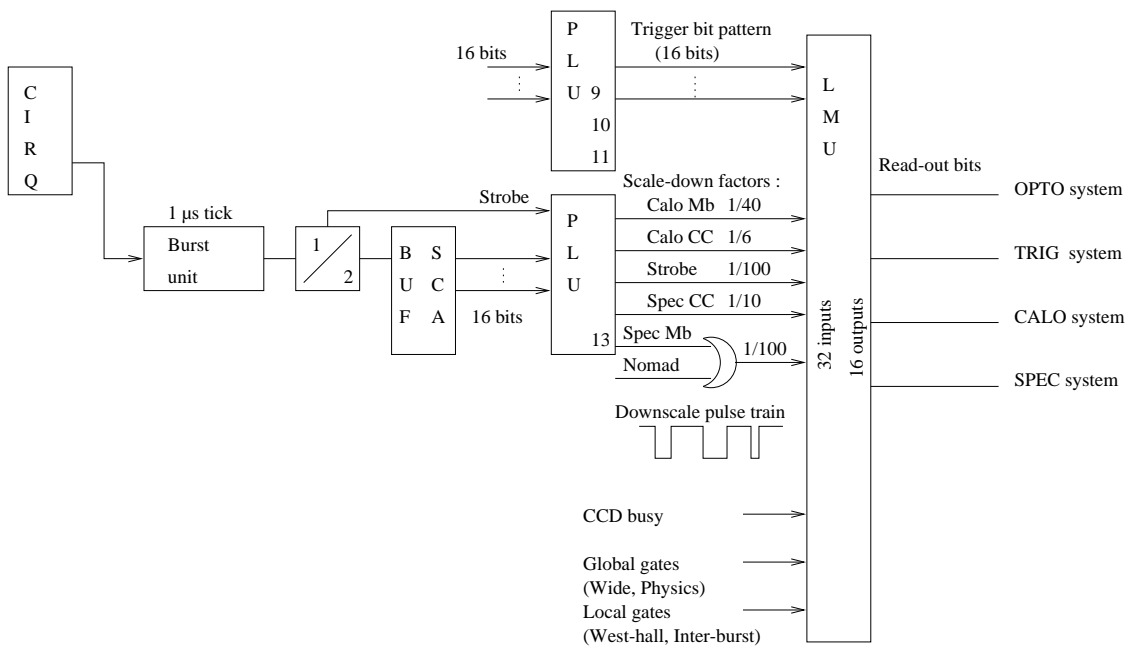


Figure 6: Schematic diagram of the generation of scaled-down triggers by the Logic Matrix Unit. The “burst unit” generates a 1 Mhz pulse-train with a pre-determined number of pulses.

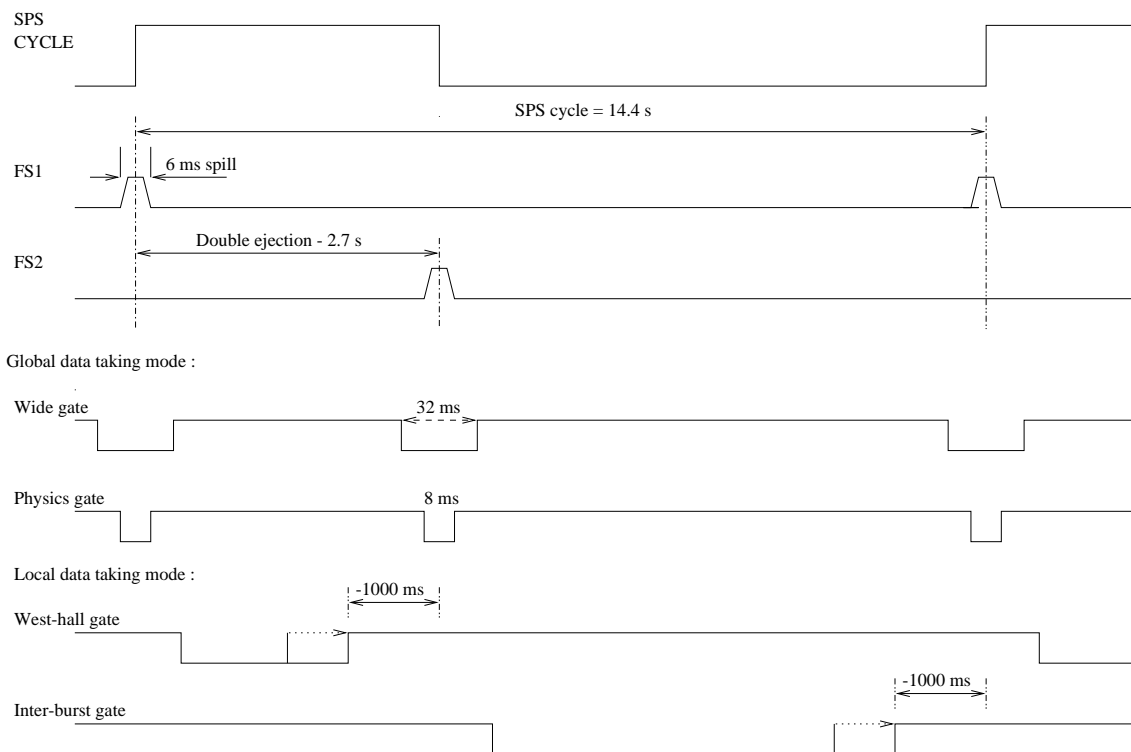


Figure 7: Illustration of main trigger functions in one data taking cycle in synchronisation with the timing structure of the CERN SPS cycle and the Wide-Band Neutrino Beam.

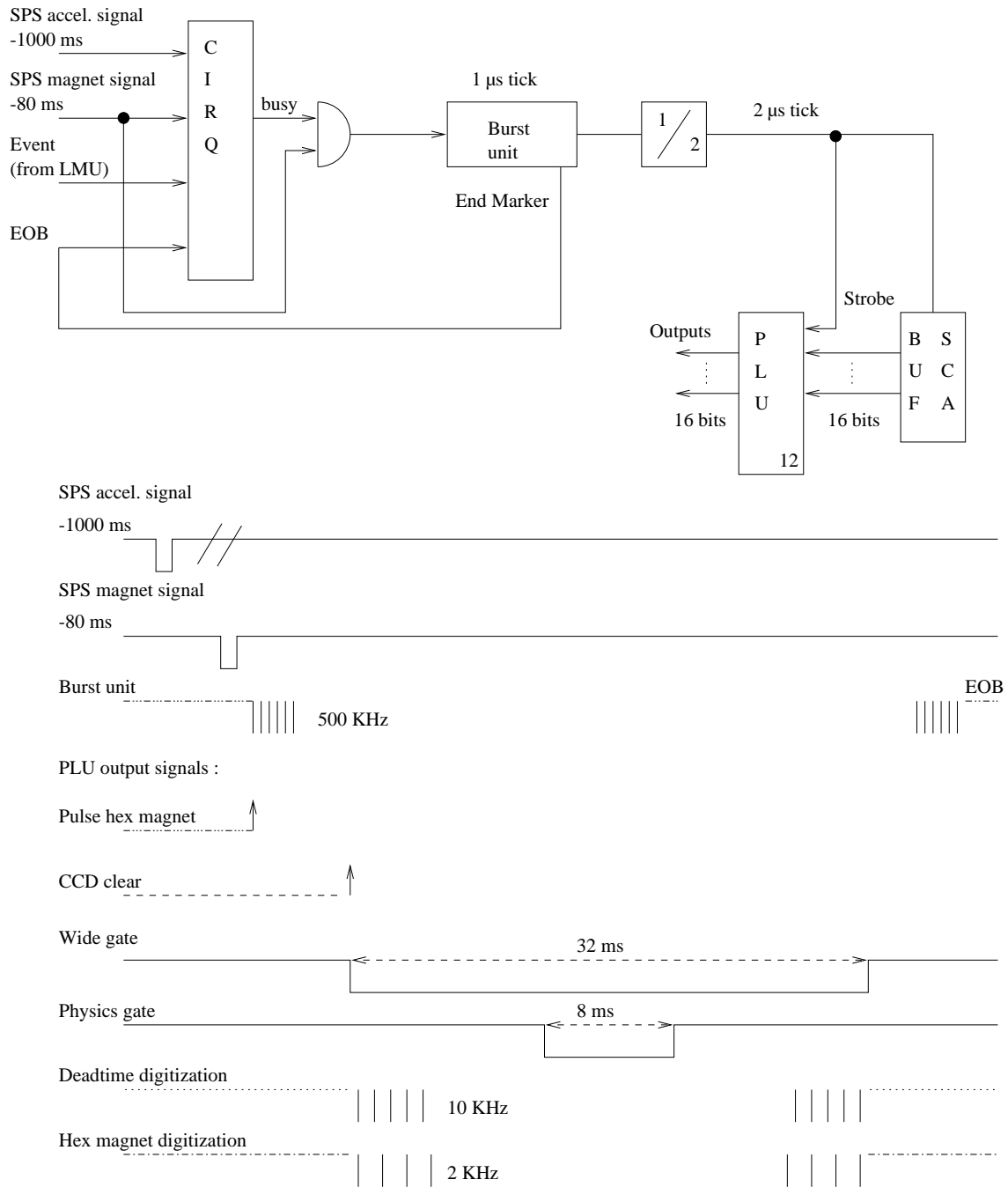


Figure 8: Schematic diagram showing the generation of gates and control signals in one neutrino spill.

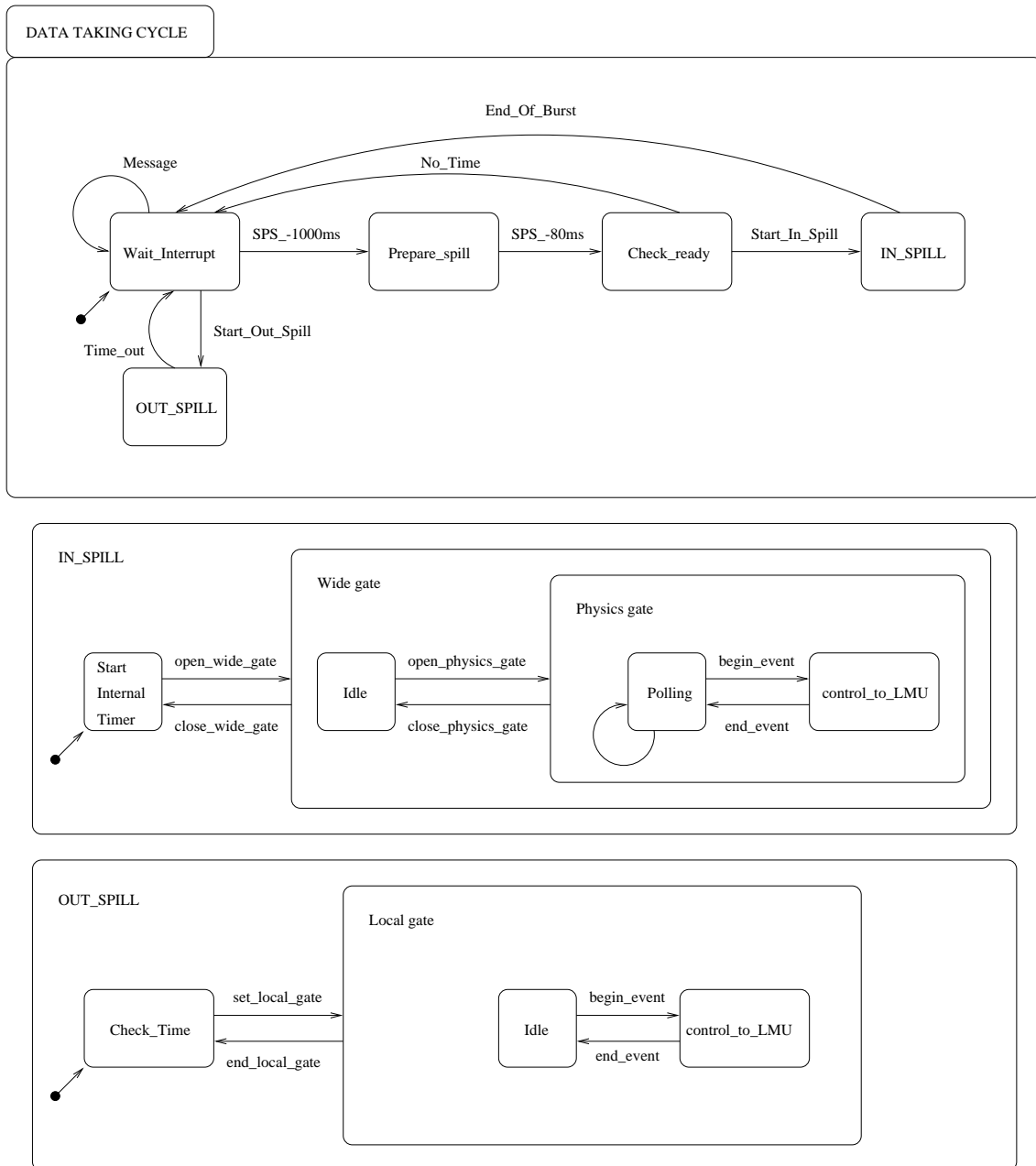


Figure 9: State machine diagram of the trigger processor during the data taking cycle. The rectangular rounded boxes identify states and arrows specify transition-actions. The IN SPILL and OUT SPILL are actually clusters of child states.

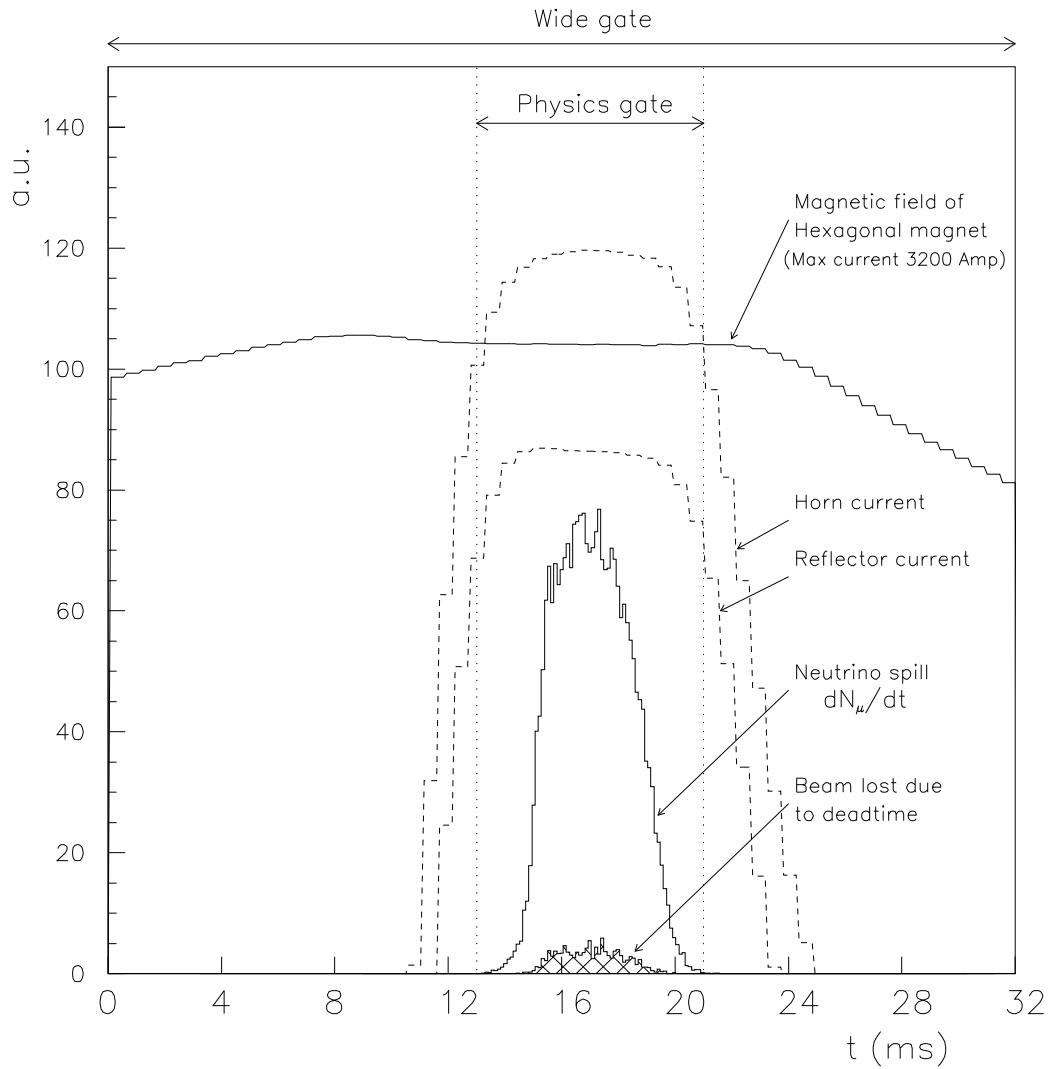


Figure 10: Online monitoring distribution of effective spill length. The figure also shows the the magnetic field of the hexagonal magnet, and the current applied to the horn and reflector focusing lenses. The data are sampled during the 32 ms “wide gate”.